



Potential of solid residues from power plants as thermochemical energy storage materials

Birgit Maaten¹ · Alar Konist¹ · Andres Siirde¹

Received: 30 November 2019 / Accepted: 12 June 2020 / Published online: 29 June 2020
© Akadémiai Kiadó, Budapest, Hungary 2020

Abstract

Due to large amounts of solid residue of oil shales produced every year by thermal processing, new ways of utilizing them are constantly investigated. As the main components of oil shale ash are calcium, magnesium and silica, the material has potential for different areas. In this paper, we investigated the possibility and potential of utilizing Estonian oil shale ash, rich in CaO, for thermochemical energy storage material. The investigated samples included the sources of main ash flow—bottom and electrostatic precipitator ash from two power plants utilizing circulating fluidized bed combustion technology. The ash from the economizer was also analysed as a comparison. The samples were characterized through elemental and chemical analysis and XRF and subjected to thermal analysis in either mixtures or pure environments of N₂ and/or CO₂.

Keywords Oil shale ash · Thermochemical energy storage · Thermal analysis · DSC · Carbonation

Introduction

Estonia is to date the only country that is still dependent on oil shale for its power production. Therefore, the properties of oil shale thermal treatment solid residues have been widely investigated [1–6]. Although both pulverized combustion (PC) and circulating fluidized bed combustion (CFBC) technologies are used, power plants utilizing pulverized combustion will be closed soon due to ageing and environmental and economic problems [2]. Oil shale is used for either oil or electricity production, and the resulting solid residues have complicated compositions. Due to the complex composition, the products of thermal treatment have been used in different fields. For example, numerous investigations have revolved around the topic of the use of these solid residues as beneficial precursors or starting materials or as fertilizers and soil remediation agents [7–9] or for the sorption of different metals or pesticides [10–13]. New fields of application need to be investigated since annually about 7 to 8 million tons of alkaline ash is being produced by oil shale burning power plants [2]. Historically, the main way of handling ash has been depositing it in ash fields, which is

still being implemented to date. We have previously shown how oil shale ash can sequester CO₂ in such natural conditions—meaning that the produced ash can bind CO₂ in the ash field where it is usually deposited, thereby producing CaCO₃ [14]. Among the most referred properties of the produced Estonian oil shale ash is the high content of calcium oxide—most reported values were in the range of up to 60% [6, 15–20]. In comparison, Tang et al. have shown the content of calcium oxide in various Chinese oil shales to remain in the range of 1.1–4.5% [21]. In contrast, Estonian oil shale has been shown to contain several times more, about 20% of calcium oxide [22]. This is a good illustration of the specialty of Estonian oil shale.

Thermochemical energy storage (TCES) is one of the categories for thermal energy storage. As described by Jahromy [23], the process is accomplished through a set of reactions—a material decomposes through an endothermic reaction, thereby producing a solid residue and a gaseous component, after which the solid residue then reacts with those gaseous component through an exothermic reaction. This produces a discharged material through the release of the stored heat, which can then be removed. Therefore, the most important requirements for a thermochemical energy storage material are its ability to store heat through endothermic reactions and the possibility of an exothermic reaction between with a gaseous component. This enables cheaper thermal energy storage with much

✉ Birgit Maaten
birgit.maaten@taltech.ee

¹ Department of Energy Technology, Tallinn University of Technology, Ehitajate tee 5, 19086 Tallinn, Estonia

less environmental encroachment—cyclic systems which are in most cases reversible are being investigated [24]. In turn, TCES materials are characterized by high energy density and zero energy loss [25]. Different materials have been investigated for TCES. For example, Korhammer et al. showed that pure salt–alcohol solvates cannot be prepared in the needed conditions [26]. Salt composites like SrCl_2 and MgSO_4 , as described by Posern and Osburg, exhibited high potential for TCES [27]. Carbonates have also been shown to be suitable candidates due to their properties like high operating temperature, non-toxic nature and high volumetric density [24]. The respective reaction systems have to match numerous requirements, and therefore, different screening approaches have been proposed to identify suitable systems [28]. As oil shale ash contains high amounts of calcium, it might be a suitable material for thermochemical energy storage, due to its ability to sequester CO_2 [14]. This was shown by Jahromy et al., due to the rich composition of oil shale ash, it is believed that ash could be used as a potential thermochemical energy storage material [23]. Sun et al. also described TCES systems based on CaO/CaCO_3 cycles with high global efficiency [29].

Alternative ways of utilizing oil shale ash are being investigated, and the purpose of this paper was to characterize different ash streams of circulating fluidized bed combustion using thermogravimetric analysis. Additionally, it was aimed at comparing the ashes of two different CFBC facilities and to map the thermochemical properties and behaviour of those industrial ashes in different gaseous environments.

This research focused on the bottom, economizer (eco) and the first field of electrostatic precipitator (ESP1) ash samples. These were chosen since ESP1 and bottom ash (BA) are the two main ash flows from the ash split and the economizer ash as the middle sampling point between the two former [18].

Experimental

Materials

The materials used in this research can be described as follows. The used oil shale ash samples were the bottom, economizer and electrostatic precipitator first field ashes from two different CFBC boilers. The boilers, which were supplied by two different boiler manufacturers—Alstom (Auvere power plant) and Foster Wheeler (Eesti power plant), have major design and technological differences. The ash samples were crushed to analytical particle size before subsequent set of analysis. Elemental analysis (Table 1) was done on an Elementar Analyser System Vario MACRO CHNS analyser. The elemental analysis was done according to standards EVS 664:2017 and EVS-ISO 29541:2015. The contents of other elements (Table 2) were analysed using Rigaku Primus II WD-XRF. The XRF analysis was done according to ISO/TS 16996:2015. The content of free calcium oxide was analysed according to a modified version of DIN 51729 part 6 chapter 2. The mineral composition of the

Table 1 Chemical composition of the used ash samples, dry basis/mass%

	C ^{total}	H	N	S ^{total}	TOC ^a	TIC ^b
Auvere bottom ash	4.12	0.26	0.04	1.46	0.49	3.63
Auvere fly ash—eco	1.84	0.21	0.04	2.41	0.12	1.72
Auvere fly ash—ESP1	1.37	0.14	0.04	2.86	0.27	1.10
Eesti PP bottom ash	8.28	0.13	0.03	1.37	0.37	7.91
Eesti PP fly ash—eco	1.30	0.18	0.05	2.93	0.0	1.30
Eesti PP fly ash—ESP1	1.64	0.16	0.04	2.28	0.24	1.40

^aTotal organic carbon, calculated by difference from total carbon and total inorganic carbon

^bTotal inorganic carbon

Table 2 Elemental composition of the used samples/mass% dry basis and specific surface area/ $\text{m}^2 \text{g}^{-1}$

	CaO_{free}	CaO	SiO_2	MgO	Al_2O_3	Fe_2O_3	K_2O	TiO_2	Na_2O	SSA ^a
Auvere bottom ash	23.2	49.70	5.88	8.15	2.19	2.66	0.67	0.12	0.030	n.d
Auvere fly ash—eco	19.3	33.86	23.57	5.40	8.36	3.72	3.52	0.48	0.122	3.4
Auvere fly ash—ESP1	20.2	36.00	22.88	5.75	8.80	3.68	3.50	0.48	0.122	3.4
Eesti PP bottom ash	6.5	45.72	6.86	4.71	2.63	2.10	0.70	0.13	0.030	5.3
Eesti PP fly ash—eco	14.65	30.36	26.65	4.95	9.54	3.70	3.28	0.51	0.101	7.8
Eesti PP fly ash—ESP1	16.6	27.53	30.03	4.67	11.01	4.00	3.92	0.60	0.111	7.0

n.d not determined

^aCalculated using the BET method

Table 3 Mineral composition of Eesti and Auvere power plant ash samples, measured with XRD/mass%

	Auvere bot- tom ash	Auvere fly ash—eco	Auvere fly ash—ESP1	Eesti PP bot- tom ash	Eesti PP fly ash—eco	Eesti PP fly ash—ESP1
Quartz	3.1	14.4	11.4	4.5	19.2	19.5
K-feldspar	2.0	14.5	14.6	2.4	11.5	13.9
Muscovite	1.4	7.0	6.1	n.d ^a	3.8	5.9
Calcite	28.3	16.2	11.4	63.5	14.3	13.9
Dolomite	3.7	n.d ^a	n.d ^a	6.0	n.d ^a	n.d ^a
Lime	2.4	1.3	2.1	n.d ^a	3.6	2.5
Portlandite	23.0	17.1	18.8	3.6	11.0	8.9
Periclase	7.8	6.1	6.9	4.2	5.8	5.1
Anhydrite	12.7	6.5	8.0	5.4	13.3	11.3
C2S	6.4	8.2	10.1	4.6	6.7	7.2
Akermanite	6.1	3.5	4.5	2.8	7.5	7.8
Merwinite	1.9	2.7	3.5	1.5	1.0	1.6
Hematite	1.0	1.8	1.7	1.5	2.0	2.2
Sylvite	n.d ^a	0.6	0.8	n.d ^a	n.d ^a	n.d ^a

^aNot detected

samples (Table 3) was analysed using a Bruker Advance D8 diffraction system equipped with a LynxEye detector.

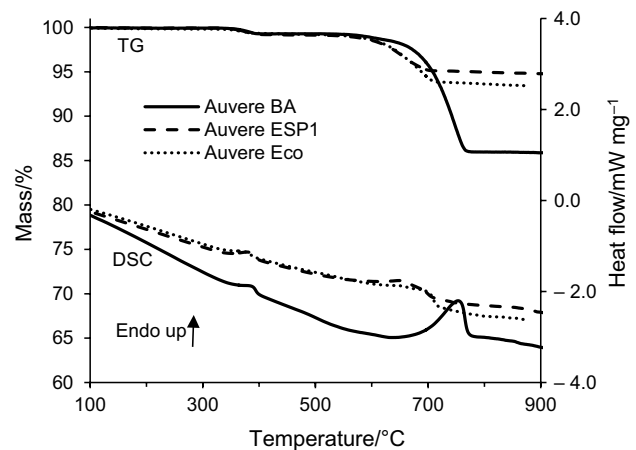
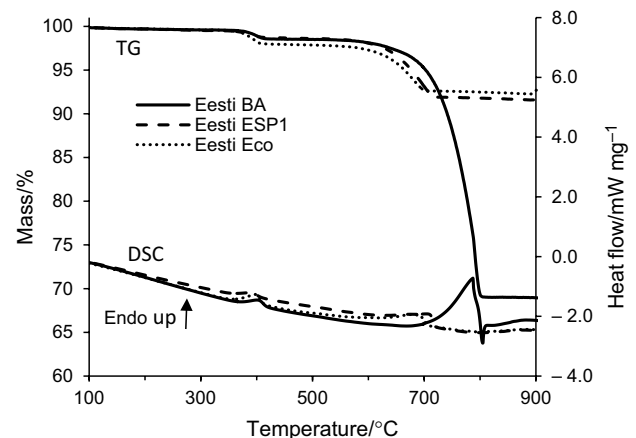
Equipment and procedure

For thermogravimetric (TG) and evaporating gas measurements, a NETZSCH STA 449 F3 Jupiter© with a water vapour furnace and differential scanning calorimetry coupled with a NETZSCH QMS Aëolos® mass spectrometer (MS) were used. The heating rate used was 10 °C min⁻¹. The atmosphere consisted of high-purity N₂ and/or CO₂. Al₂O₃ crucibles without lids were used. Approximately 20 ± 2 mg of oil shale ash sample was used for the TG analysis. All measurements were performed at least twice for sufficient reproducibility.

Results and discussion

The potential for TCES is usually analysed mostly through calorimetry. In this study, thermogravimetric analysis with differential scanning calorimetry (DSC) was employed to study the properties of the ash samples. First, the samples were analysed in a nitrogen environment. The results are shown in Figs. 1 and 2.

As can be seen from Fig. 1, the thermoanalytical curves (TG curves) for ash samples from Auvere power plant showed two mass loss steps—one in the temperature range of 360–420 °C and the second in the temperature range of 550–780 °C. The first step was attributed to the dehydration of minerals and the decomposition of some residual organic matter as the samples had some organic carbon (up to 0.5 mass%, Table 1). The second step exhibited the

**Fig. 1** TG curves for Auvere PP ash samples in a N₂ environment**Fig. 2** TG curves for Eesti PP ash samples in a N₂ environment

decomposition of carbonate minerals. The results are in very good agreement with the total inorganic carbon results (Table 1), as the mass loss for carbonate minerals was about 13 mass% for bottom ash and the respective CO_2 from inorganic carbon calculated to 13.3%. For ESP1 and economizer ash samples, the amount of carbonate minerals was much smaller, around 5–7 mass%. This was illustrated by the TIC content. This difference in TIC was to be expected as the bottom ash usually exhibits the highest content of inorganic carbon with it decreasing along the flow sheet of the boiler [30]. In case of DSC, two endothermic peaks were noticed, respectively, for the same temperature ranges.

Figure 2 presents the same ash samples from Eesti power plant.

Based on the experimental data obtained, the results were generally similar to those of Auvere power plant. The only exception is the inorganic carbon content of the bottom ash—in case of Auvere power plant, the bottom ash exhibited a mass loss of almost 30 mass% for the decomposition of carbonate minerals. The extent of decomposition of carbonate minerals between the two power plants is different due to differences in the technologies. Although both power plants utilized circulating fluidized bed combustion technology, the processing temperatures were somewhat different, namely Eesti power plant used lower temperatures, thereby resulting in lower extent of carbonate mineral decomposition. This is supported by the XRD results—as can be seen from Table 3, samples from Eesti power plant exhibited much higher CaCO_3 contents than the respective samples from Auvere. The differences between TIC values and carbonate mineral compositions in Tables 2 and 3 were based on two aspects. First, XRD is unable to identify amorphous phases, which are present in the ash. Second, as the samples were stored in containers, which contained

some air, the compositions have changed during some time. This is supported by the findings of Mõtlep and co-workers who investigated Estonian semi-coke [31]. They found that already in 2 weeks of ambient condition, the calcite content was increased by nearly 4%. Additionally, the fuel preparation and velocities of gases were different as well. Namely, in Eesti power plant the fuel particles were smaller and the velocities greater than those in Auvere power plant. Another difference is the use of cyclone separators—in case of Foster Wheeler systems the cyclones are water-cooled, whereas in Alstom systems the separators are not cooled.

In order to further explain the effects occurring during the analysis, mass spectrometry was used to identify the evaporating gases. The results of water and CO_2 evaporation are shown in Fig. 3.

As can be seen from Fig. 3, in both cases the first mass loss step was mostly attributed to the evaporation of water (mass-to-charge ratio, m/z values of 17 and 18), while CO_2 (m/z 44, for size consideration shown only for Auvere BA) evaporated only during the decomposition of carbonate minerals, thereby confirming the hypothesis that the first mass loss step was mainly the result of the dehydration of some minerals. Additionally, it can be noticed that for Auvere bottom ash, the mass loss for the first step was significantly larger than those observed in Fig. 1. This was attributed to the fact that during time the hydration of lime occurred and therefore the first mass loss step increased about 3.5%. For Eesti PP bottom ash, the increase in water content was only about 0.5%. This is to be expected as the free CaO content (Table 1) of Auvere PP bottom ash is much higher than for Eesti PP bottom ash.

Similar experiments were also run in a carbon dioxide environment. The results for Auvere power plant ash samples are shown in Fig. 4 and for Eesti power plant in Fig. 5.

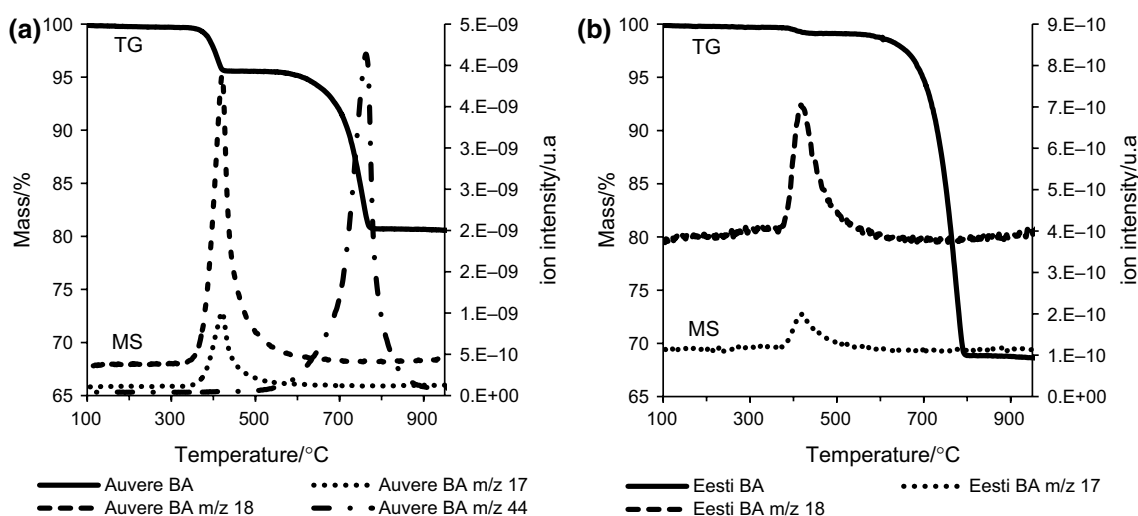


Fig. 3 Mass spectrometry results for the evaporation of water and CO_2 for Auvere (a) and Eesti PP (b) bottom ash samples

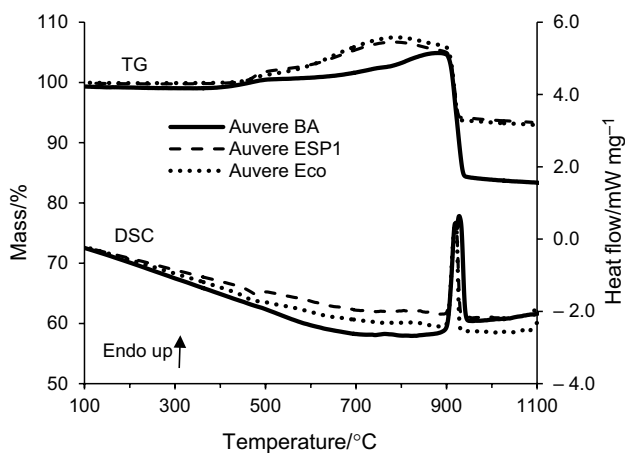


Fig. 4 TG curves for Auvere PP ash samples in a CO₂ environment

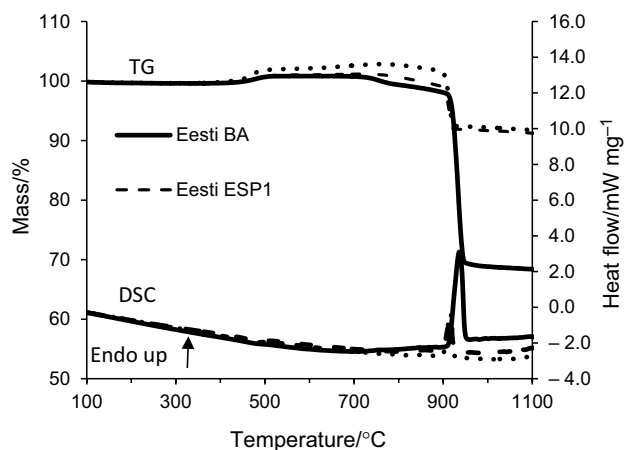


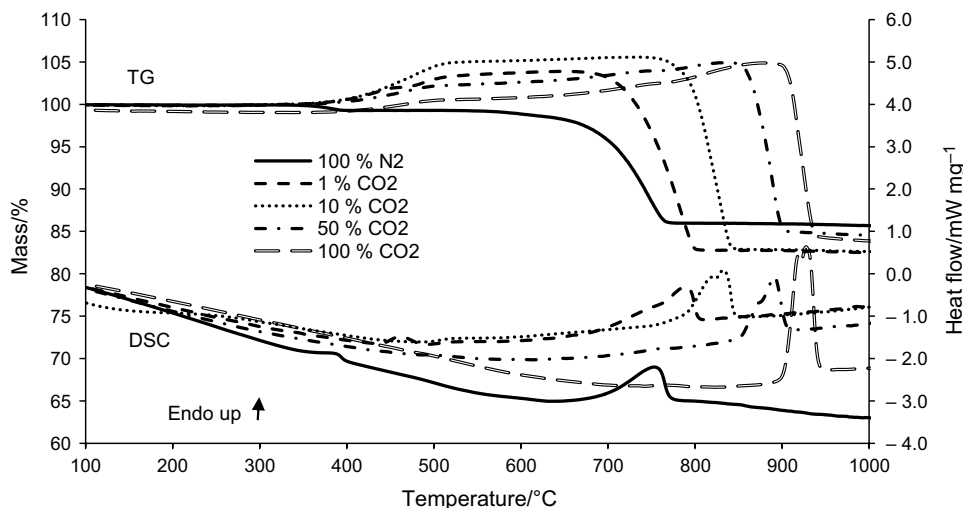
Fig. 5 TG curves for Eesti PP ash samples in a CO₂ environment

In the environment of dry carbon dioxide, the carbonation of calcium oxide occurs due to the high content of

calcium oxide in the samples [32]. This is very well visualized in Figs. 4 and 5. Namely, in Fig. 4, it can be seen that for the Auvere samples there is a major difference in the thermal behaviour of bottom ash and ESP1 and economizer ashes. For the bottom ash, the uptake of CO₂ started at a temperature of about 410 °C, reached 1.6% and stabilized at 530 °C. Further on, the uptake continued at temperatures above 600 °C and reached a maximum of 6% near 890 °C. This was followed by the decomposition of the formed and inherent carbonate minerals with the residual mass being similar to that reached in a nitrogen environment. For the ESP1 and economizer ash samples, the TG curves had a somewhat different shape. The maximal uptake reached a higher value at a lower temperature than for the bottom ash sample (7.5% at 770 °C, respectively). The capacity to sequester CO₂ has been found to be directly proportional to the amount of binary oxides (like CaO and MgO, both found in the analysed samples) and the respective hydroxides found in the matrix [32]. Additionally, according to the Stenoir formula, the maximum CO₂ uptake can be calculated by the chemical composition of the sample—namely amounts of CaO (in not bound forms), Na₂O and K₂O [33]. For the DSC measurements, only an endothermic peak for the decomposition of carbonate minerals was detected.

As visualized in Fig. 5, the samples from Eesti power plant exhibited results that were quite similar. Compared to Auvere samples, the uptake of CO₂ started at a similar temperature for the Eesti power plant samples. For Eesti power plant samples, the mass gain remained more modest—the highest mass gain was noticed for the economizer ash with the respective value of 2.8%. The bottom ash exhibited a mass gain of only 1.2%. Interestingly, a small mass loss was noticed already at temperatures of 720 °C with the main carbonate mineral decomposition step starting at temperatures of around 900 °C. The differences between the samples were attributed to differences in the composition—as can be seen

Fig. 6 Effect of CO₂ concentration on the TG curve of Auvere bottom ash



from Table 2, the samples from Eesti power plant contained somewhat less CaO, significantly less free CaO, somewhat more SiO₂ and had larger specific surface area values.

As demonstrated by Jahromy [23], for municipal solid waste incineration ash the TG-DSC analysis showed the occurrence of, depending on the sample, three to four mass loss steps and the respective peaks in DSC were also noticed. As a result, it was calculated that energy contents of up to 394 kJ kg⁻¹ were reached. Although based on the composition presented in Table 2, the initial conditions, namely a high concentration of calcium, for oil shale ash to be a candidate for TCES are present in the samples investigated in this paper, the samples did not exhibit similar thermal degradation behaviour. Only the dehydration of certain minerals, possibly gypsum, was noticed, and no other effects were present. The reason might lie in the difference in the composition of the samples. Compared to data exhibited by Jahromy, the samples investigated in this paper contained less Na₂O, SiO₂ and Al₂O₃ and significantly more CaO. As the latter is usually the main component described in the literature, it can be concluded that other components, and their possible interactions, have a notable effect on the outcome as well. Therefore, the results presented in this paper did not show potential for oil shale ash to be considered as a possible TCES material. However, the reactivity and the possible increase in CaO content should be further investigated.

As a further step, preliminary tests for the effect of CO₂ were run for Auvere bottom ash. The results are shown in Fig. 6.

As visualized in Fig. 6, the effect of CO₂ is significant. The process is highly dependent on the partial pressure of CO₂—the more the CO₂ is involved, the higher the decomposition temperatures compared to a pure nitrogen environment. Additionally, already the use of one per cent of CO₂ eliminated the step of dehydration of minerals and the carbonation of the sample occurred already at such a low concentration. For all the tests run with some amount of CO₂ in the environment, the maximum mass gain remained quite similar. Enriching the environment with CO₂ resulted in the increase in the decomposition temperature by nearly 200 °C. This was a good example of how and to which extent the choice of gaseous environment affected the thermal analysis results.

Conclusions

This paper investigated the thermal behaviour of ash samples from two circulating fluidized bed combustion facilities in nitrogen and/or carbon dioxide environments. The samples exhibited different compositions and therefore different behaviour profiles during thermal treatment. The samples

from Auvere power plant contained significantly more free calcium oxide than the respective samples from Eesti power plant. The samples from Auvere and Eesti power plant exhibited similar thermal decomposition profiles in nitrogen with the main difference being only the amount of carbonate minerals. Running the analysis in a carbon dioxide environment resulted in the carbonation of the samples due to the high amounts of calcium oxide. The samples from Eesti power plant showed a smaller mass gain when compared to samples from Auvere power plant. The differences were attributed to the differences in the operating temperatures of the two power plants, which in turn affect the composition of the formed solid residues. Generally, the potential for TCES was found to be scarce.

Acknowledgements This work was supported by the Estonian Research Council Grant (PSG266).

References

1. Arro H, Prikk A, Pihu T, Öpik I. Utilization of semi-coke of Estonian shale oil industry. *Oil Shale*. 2002;19:117–25.
2. Pihu T, Konist A, Puura E, Liira M, Kirsimäe K. Properties and environmental impact of oil shale ash landfills. *Oil Shale*. 2019;36:257–70.
3. Bitjukova L, Mõtsep R, Kirsimäe K. Composition of oil shale ashes from pulverized firing and circulating fluidized-bed boiler in Narva thermal power plants, Estonia. *Oil Shale*. 2010;27:339–53.
4. Paat A. About the mineralogical composition of Estonian oil shale ash. *Oil Shale*. 2002;19:321–33.
5. Laja M, Urb G, Irha N, Reinik J, Kirso U. Leaching behavior of ash fractions from oil shale combustion by fluidized bed and pulverized firing processes. *Oil Shale*. 2006;22:453–65.
6. Konist A, Valtsev A, Loo L, Pihu T, Liira M, Kirsimäe K. Influence of oxy-fuel combustion of Ca-rich oil shale fuel on carbonate stability and ash composition. *Fuel*. 2015;139:671–7.
7. Trass O, Kuusik R, Kaljuvee T. Activation of oil shale ashes for sulfur capture. *Oil Shale*. 2018;35:375–85.
8. Wei H, Zhang Y, Cui J, Han L, Li Z. Engineering and environmental evaluation of silty clay modified by waste fly ash and oil shale ash as a road subgrade material. *Constr Build Mater*. 2019;196:204–13.
9. Triisberg-Uljas T, Vellak K, Karofeld E. Application of oil-shale ash and straw mulch promotes the revegetation of extracted peatlands. *Ecol Eng*. 2018;110:99–106.
10. Shawabkeh R, Al-Harashsheh A, Al-Otoom A. Copper and zinc sorption by treated oil shale ash. *Sep Purif Technol*. 2004;40:251–7.
11. Zhu BL, Xiu ZM, Liu N, Bi HT, Lv CX. Adsorption of lead and cadmium ions from aqueous solutions by modified oil shale ash. *Oil Shale*. 2012;29:268–78.
12. Al-Qodah Z, Shawaqfeh AT, Lafi WK. Adsorption of pesticides from aqueous solutions using oil shale ash. *Desalination*. 2007;208:294–305.
13. Al-Qodah Z. Adsorption of dyes using shale oil ash. *Water Res*. 2000;34:4295–303.
14. Konist A, Maaten B, Loo L, Neshumayev D, Pihu T. Mineral sequestration of CO₂ by carbonation of Ca-rich oil shale ash in natural conditions. *Oil Shale*. 2016;33:248–59.

15. Konist A, Pihu T, Neshumayev D, Külaots I. Low grade fuel oil shale and biomass Co-combustion in CFB boiler. *Oil Shale*. 2013;30:294.
16. Pihu T, Konist A, Neshumayev D, Loosaar J, Siirde A, Parve T, et al. Short-term tests on firing oil shale fuel applying low-temperature vortex technology. *Oil Shale*. 2012;29:3–17.
17. Neshumayev D, Pihu T, Siirde A, Järvik O, Konist A. Solid heat carrier oil shale retorting technology with integrated CFB technology. *Oil Shale*. 2019;36:99–113.
18. Plamus K, Soosaar S, Ots A, Neshumayev D. Firing Estonian oil shale of higher quality in CFB boilers: environmental and economic impact. *Oil Shale*. 2011;28:113.
19. Saether OM, Banks D, Kirso U, Bitjukova L, Sorlie JE. The chemistry and mineralogy of waste from retorting and combustion of oil shale. *Geol Soc Lond, Spec Publ*. 2004;236:263–84.
20. Konist A, Pihu T, Neshumayev D, Siirde A. Oil shale pulverized firing: boiler efficiency, ash balance and flue gas composition. *Oil Shale*. 2013;30:6.
21. Tang L, Yan Y, Meng Y, Wang J, Jiang P, Pang CH, et al. CO₂ gasification and pyrolysis reactivity evaluation of oil shale. *Energy Procedia*. 2019;158:1694–9.
22. Loo L, Maaten B, Neshumayev D, Konist A. Oxygen influence on Estonian kukersite oil shale devolatilization and char combustion. *Oil Shale*. 2017;34:219–31.
23. Setoodeh Jahromy S, Jordan C, Harasek M, Werner A, Winter F, Azam M, et al. Fly ash from municipal solid waste incineration as a potential thermochemical energy storage material. *Energy & Fuels*. 2019;33:5810–9.
24. Sunku Prasad J, Muthukumar P, Desai F, Basu DN, Rahman MM. A critical review of high-temperature reversible thermochemical energy storage systems. *Appl Energy*. 2019;254:113733–54.
25. Abedin AH, Rosen MA. A critical review of thermochemical energy storage systems. *Open Renew Energy J*. 2011;4:42–6.
26. Korhammer K, Mihály J, Bálint S, Trif L, Vass Á, Tompos A, et al. Reversible formation of alcohol solvates and their potential use for heat storage. *J Therm Anal Calorim*. 2019;138:11–33.
27. Posern K, Osburg A. Determination of the heat storage performance of thermochemical heat storage materials based on SrCl₂ and MgSO₄. *J Therm Anal Calorim*. 2018;131:2769–73.
28. Afflerbach S, Trettin R. A systematic screening approach for new materials for thermochemical energy storage and conversion based on the Strunz mineral classification system. *Thermochim Acta*. 2019;674:82–94.
29. Sun H, Li Y, Bian Z, Yan X, Wang Z, Liu W. Thermochemical energy storage performances of Ca-based natural and waste materials under high pressure during CaO/CaCO₃ cycles. *Energy Convers Manag*. 2019;197:111885–94.
30. Kuusik R, Uibu M, Kirsimäe K. Characterization of oil shale ashes formed at industrial-scale CFBC boilers. *Oil Shale*. 2006;22:407–19.
31. Mõtlep R, Kirsimäe K, Talviste P, Puura E, Jürgenson J. Mineral composition of Estonian oil shale semi-coke sediments. *Oil Shale*. 2007;24:405–22.
32. Dindi A, Quang DV, Vega LF, Nashef E, Abu-Zahra MRM. Applications of fly ash for CO₂ capture, utilization, and storage. *J CO₂ Util*. 2019;29:82–102.
33. Nyambura MG, Mugeru GW, Felicia PL, Gathura NP. Carbonation of brine impacted fractionated coal fly ash: implications for CO₂ sequestration. *J Environ Manag*. 2011;92:655–64.

Publisher's Note Springer Nature remains neutral with regard to jurisdictional claims in published maps and institutional affiliations.